

5

ADA131238

NEW METHOD IN ELEMENTARY PARTICLE DETECTION

Final Report

Contract F49620-81-C-0024

ARPA Order 4099

Program Code 1A 10

DTIC  
ELECTE  
AUG 10 1983  
S D D



Approved for public release  
distribution unlimited.

DTIC FILE COPY

UNIVERSITY OF MARYLAND  
DEPARTMENT OF PHYSICS AND ASTRONOMY  
COLLEGE PARK, MARYLAND

83 08 08 078

# UNCLASSIFIED

SECURITY CLASSIFICATION OF THIS PAGE (When Data Entered)

| REPORT DOCUMENTATION PAGE  |  | READ INSTRUCTIONS<br>BEFORE COMPLETING FORM   |
|--|--|---|
| 1. REPORT NUMBER<br><b>AFOSR-TR- 83-0681</b>   | 2. GOVT ACCESSION NO.<br><i>AD-A131238</i> | 3. RECIPIENT'S CATALOG NUMBER   |
| 4. TITLE (and Subtitle)<br><br>NEW METHOD IN ELEMENTARY PARTICLE DETECTION   |  | 5. TYPE OF REPORT & PERIOD COVERED<br>Final Report<br>1/1/81 - 12/31/82                                     |
| 7. AUTHOR(s)<br><br>J. Weber   |  | 6. PERFORMING ORG. REPORT NUMBER  |
| 9. PERFORMING ORGANIZATION NAME AND ADDRESS<br>Department of Physics and Astronomy<br>University of Maryland<br>College Park, Maryland 20742   |  | 8. CONTRACT OR GRANT NUMBER(s)<br><br>F-49620-81-C-0024   |
| 11. CONTROLLING OFFICE NAME AND ADDRESS<br>Air Force Office of Scientific Research<br>Bolling Air Force Base<br>Washington, D.C. 20332   |  | 10. PROGRAM ELEMENT, PROJECT, TASK<br>AREA & WORK UNIT NUMBERS<br><br>ARPA Order 4099<br>Program Code 1A 10 |
| 14. MONITORING AGENCY NAME & ADDRESS (if different from Controlling Office)<br>Defense Advanced Research Projects Agency<br>1400 Wilson Boulevard<br>Arlington, Virginia 22209   |  | 12. REPORT DATE<br>February 1983  |
| 16. DISTRIBUTION STATEMENT (of this Report)<br><br><br><p style="text-align: center;">Approved for public release;<br/>distribution unlimited.</p>   |  | 13. NUMBER OF PAGES   |
| 17. DISTRIBUTION STATEMENT (of the abstract entered in Block 20, if different from Report)   |  | 15. SECURITY CLASS. (of this report)<br><br>Unclassified  |
| 18. SUPPLEMENTARY NOTES  |  | 15a. DECLASSIFICATION/DOWNGRADING<br>SCHEDULE   |
| 19. KEY WORDS (Continue on reverse side if necessary and identify by block number)<br><br>Coherent Scattering, Elementary Particle Detection   |  |   |
| 20. ABSTRACT (Continue on reverse side if necessary and identify by block number)<br><br>A general theory of coherent scattering is presented. Applications for very low energy involving the neutral current interactions are considered in detail, together with results of experimental checks. |  |   |

ABSTRACT

A general theory of coherent scattering is presented. Applications for very low energy involving the neutral current interactions are considered in detail, together with results of experimental checks.

|                    |                                     |
|--------------------|-------------------------------------|
| Accession For      |                                     |
| NTIS GRA&I         | <input checked="" type="checkbox"/> |
| DTIC TAB           | <input type="checkbox"/>            |
| Unannounced        | <input type="checkbox"/>            |
| Justification      |                                     |
| By _____           |                                     |
| Distribution/      |                                     |
| Availability Codes |                                     |
| Dist               | Avail and/or<br>Special             |
| A                  |                                     |



AIR FORCE OFFICE OF SCIENTIFIC RESEARCH (AFSC)  
NOTICE OF TRANSMITTAL TO DTIC  
This technical report has been reviewed and is approved for public release IAW AFR 190-12. Distribution is unlimited.  
MATTHEW J. KEEPER  
Chief, Technical Information Division

## Introduction

Coherent and incoherent scattering have been studied for several generations. For the scattering of Xrays by the electrons in a crystal, large peaks resulting from coherent scattering are observed. If an ionization chamber is employed for observation of the scattered Xrays, it subtends a solid angle considerably larger than the solid angle of an intensity peak. The integrated intensity observed under these conditions is a measure of the total cross section. It is stated in the classic work<sup>1</sup> of Compton and Allison that "in this case the intensity of scattering by  $N$  atoms is just  $N$  times that scattered by a single atom".

Thomson scattering, according to classical electromagnetic theory, gives the result that for scattering by a number of charges in a region small compared with a wavelength, the total cross section is proportional to the square of the number of scatterers.<sup>2</sup> For the opposite limit, where the average spacing of the scatterers is many wavelengths, the total cross section<sup>3</sup> is proportional to the number of scatterers. Indeed, it appears usually to be true, that for wavelengths small compared with scatterer spacing, the effects of constructive and destructive interference over all solid angles give a total cross section much smaller, than the cross section of a single scatterer multiplied by the square of the number of scatterers.

For a large number of scatterers, the total cross section depends on the interaction of the scatterers with the incident radiation and with each other. The important issue explored in

this paper is the following one:

Can the interaction of scatterers with each other be specified such that the total cross section is very large for incident wavelength small compared with the scatterer spacing?

If materials exist or can be synthesized with the required properties, these would serve for detection of the kinds of radiation for which sensitive detectors do not now exist.

Detailed investigation of momentum energy exchange which follows, gives a solution with large cross sections and the required material properties.

This solution is applied to develop an entirely new method for neutrino detection. An experiment is described which appears to give unusually large total cross sections.

#### Momentum-Energy Exchange Possibilities

When radiation interacts with a number of scatterers, it may be possible to make observations to determine that an individual scatterer exchanged all of the energy-momentum. For this case, each scatterer appears to act independently of the others, and interference effects are not observed. In other experiments, an entire ensemble may exchange energy-momentum without possibility of determining which scatterer or scatterers transmitted the exchange to the ensemble. Interference effects are then observed.

There are many ways in which the total energy-momentum may be exchanged. For example  $N$  scatterers might each exchange momentum  $\frac{\Delta \bar{p}}{N}$  for a total exchange  $\Delta \bar{p}$ , or different particles might exchange different amounts such that the vector

sum is  $\Delta \bar{p}$  .

Here we explore the consequences of assuming that the entire energy-momentum is exchanged by one scatterer. The ensemble of scatterers is assumed to be so tightly bound that the subsequent observations cannot reveal which scatterer transmitted the exchange.

### Interaction of Four Current Densities

Let us consider the S matrix for interaction of two four current densities<sup>4,5</sup> given by

$$S = \frac{i}{\hbar c} \int \langle F | \bar{\psi}_S \Gamma \psi_S \bar{\psi}_I K \psi_I | 0 \rangle d^4x \quad (1)$$

F is the final state, 0 is the original state.  $\bar{\psi}_S$  is a creation operator for scatterer S,  $\bar{\psi}_I$  is a creation operator for incident particle I.  $\psi_S$  and  $\psi_I$  are the corresponding annihilation operators.  $\Gamma$  and K are position independent operators.

The operators  $\bar{\psi}_S$  and  $\bar{\psi}_I$  are represented by the following expansions:

$$\begin{aligned} \bar{\psi}_S &= \sum_n \sum_j \psi_{Sjn}^* (\bar{r} - \bar{r}_n) a_{jn}^\dagger \\ \bar{\psi}_I &= \frac{1}{\sqrt{V}} \sum_k \bar{u}_{Ik} e^{-\frac{i}{\hbar} \bar{p}_{Ik} \cdot \bar{r}} d_k^\dagger \end{aligned} \quad (2)$$

In (2)  $\bar{r}$  is the position three vector,  $a_{jn}^\dagger$  is a

In the Mossbauer effect<sup>6,9,10</sup> an atomic nucleus emits a gamma ray. For a significant fraction of these emissions the entire crystal recoils. In principle the nuclear quantum state of every atom could be determined prior to the emission of the gamma ray, and the identity of the emitter established by subsequent measurements.

For the scattering discussed in this paper, the identity of the scatterer cannot be determined. Any of the scattering processes in which momentum is transferred to many scatterers would result in recoil of the entire crystal if its Debye temperature is very high. Only one of these many processes - in which the entire scattering momentum is transferred to one unidentified nucleus - is being considered here.

creation operator for the state with wavefunction  $\psi_{sjn}^*$ ,  
 $n$  refers to the  $n^{\text{th}}$  scattering site.  $a_k^\dagger$  is a creation  
operator for an incident particle with known  
momentum  $\bar{p}_{Ik}$ .  $U_{Ik}$  is an incident particle  
spinor.

Let there be  $N$  scatterers in a solid. For the  
states  $\psi_{sjn}$ , harmonic oscillator states are selected. For  
a harmonic oscillator wavefunction centered at radius vector  $\bar{r}_n$

$$\psi_{so_n} = \left(\frac{\mu}{\pi}\right)^{3/2} e^{-\mu |\bar{r} - \bar{r}_n|^2} \quad (3)$$

In (3)  $\mu$  specifies the volume of each scatterer. For the  $N$   
scatterers, the original state is taken to be

$$a_{o_1}^\dagger a_{o_2}^\dagger a_{o_3}^\dagger \dots a_{o_N}^\dagger \left| \begin{array}{l} \text{VACUUM} \\ \text{STATE} \end{array} \right\rangle \quad (4)$$

For nuclei in a solid, the wavefunctions of different scatterers  
will not overlap to a significant degree, and the symmetry of the  
many particle wavefunction need not be considered.

Let us assume now that the scatterer position probability  
distribution  $\psi_{sjn}^* \psi_{sjn}$  is not changed by the scattering,

$$(\psi_{Sj_n}^* \psi_{Sj_n})_{\text{BEFORE SCATTERING}} = (\psi_{Sj_n}^* \psi_{Sj_n})_{\text{AFTER SCATTERING}} \quad (5)$$

(5) implies that each final scatterer state  $(\psi_{Sj_n})_F$  is related to the original state by

$$(\psi_{Sj_n})_F = (\psi_{Sj_n})_0 e^{i\Delta p_n x^n / \hbar} \quad (6)$$

(6) implies that each component in the momentum decomposition of the scatterer is shifted by the three momentum  $\Delta \vec{p}$ , corresponding to momentum exchange  $\Delta \vec{p}$ .

Suppose there is exchange of momentum  $\Delta p_n$  at the  $n^{\text{th}}$  site, from (6)  $\psi_S$  in (2) must be replaced by

$$\bar{\psi}'_S = \psi_{S0n}^* a_{0n}^+ e^{-i\Delta p_n x^n / \hbar} + \sum_{i \neq n} \psi_{S0i}^* a_{0i}^+ \quad (7)$$

We may write (7) in a more illuminating form by

adding  $\psi_{S0n}^* a_{0n}^+$  to the last term and subtracting it from the first term to give

$$\bar{\Psi}'_s = \Psi_{son}^* a_{on}^+ \left[ e^{-\frac{i\Delta p_n X^n}{\hbar}} - 1 \right] + \sum_{ALL N} \Psi_{soi}^* a_{oi}^+ \quad (8)$$

In (8) the last term is the probability amplitude for the possible process where no momentum is exchanged at any site. The first term then gives the contribution to the amplitude for exchange  $\Delta p_n$  at the  $n^{\text{th}}$  site. Since we are assuming strong coupling of nuclei to each other with no possibility of identifying the scattering site, we must sum only the first term in (8) over all possible sites.

This gives, for collective momentum transfer phase shift scattering

$$S = \frac{\bar{U}_{IF} K U_{IO}}{\hbar c V} \int \sum_{n=1}^{n=N} \left( \frac{K}{\pi} \right)^{3/2} e^{-K|\bar{\pi} - \bar{\pi}_n|^2 + \frac{i}{\hbar} (p_{IO} - p_{IF} - \Delta p)_r X^n} d^3 X \quad (9)$$

### Scattering Cross Sections

Suppose now that we have nuclei in a cubic crystal with  $N$  identical cells each with length  $a$ . For these assumptions the  $S$  matrix (9) for initial and final states in which the harmonic oscillator quantum numbers are the same, is given by

$$S = \bar{U}_{IF} K U_{IO} X Y Z T \left( \frac{1}{\hbar V} \right) \quad (10)$$

with

$$X = \sum_{n=1}^{n=N^{1/3}} e^{\frac{i}{\hbar} (P_{IO} - P_{IF} - \Delta p)_x X_n - \frac{1}{\kappa} \left( \frac{P_{IO} - P_{IF} - \Delta p}{2\hbar} \right)_x^2}$$

In (10)  $X_n = na$ , with corresponding definitions for Y and Z. As before,  $\kappa$  is a parameter specifying the width of the harmonic oscillator wavefunction.

$$T = \frac{\text{slh} \left[ \frac{(E_{IF} - E_{IO} + E_{SF} - E_{SO}) \tau}{2\hbar} \right]}{\left[ \frac{E_{IF} - E_{IO} + E_{SF} - E_{SO}}{2\hbar} \right]} \quad (11)$$

$E_{IF}$  and  $E_{SF}$  are the final state energies of the incident particle and ensemble of scatterers respectively,  $E_{IO}$  and  $E_{SO}$  are the corresponding original energies.

The scattering cross section is given by  $\sigma$ , with

$$\sigma = \sum \frac{V(S-1)^2}{c\tau} = \frac{V}{(2\pi)^4 c^2 \hbar^8} \int \left| \bar{U}_{IF} K U_{IO} X Y Z T \right|^2 d\bar{p}_S d\bar{p}_I \quad (12)$$

In (12)  $d\bar{p}_s$  is the element of momentum space for the final state of the ensemble of scatterers,  $d\bar{p}_I$  is the element of momentum space for the final state of the incident particle.  $T$  in (11) and (12) is a function of the momentum variables in  $X$ ,  $Y$ , and  $Z$ . The integration (12) is carried out in the following way:

The length  $L$  of the crystal is given by  $L = aN^{1/3}$ , to a very good approximation we may evaluate

$$\frac{L}{2\pi\hbar} \int X^2 d p_{sx} = \frac{L}{2\pi\hbar} \int \left[ \frac{\sin \frac{N^{1/3} a [p_{I0} - p_{IF} - \Delta p]_x}{2\hbar}}{\sin \frac{a [p_{I0} - p_{IF} - \Delta p]_x}{2\hbar}} \right]^2 e^{-\frac{2}{\hbar} \left( \frac{p_{I0} - p_{IF} - \Delta p \right)^2} {2\hbar}} d p_{sx} = N^{2/3} \quad (13)$$

Combining (13), (12) and (11) then gives

$$\sigma = \frac{N^2}{(2\pi)^3 c \hbar^5 \epsilon} \int (\bar{U}_{IF} K U_{I0} T)^2 d p_I = \frac{N^2}{(2\pi)^3 c \hbar^5 \epsilon} \int (\bar{U}_{IF} K U_{I0} T p_I)^2 \frac{d |p_I| dE d\Omega_I}{dE} \quad (14)$$

with  $E = E_I + E_S$ ,  $d\Omega_I$  is the element of solid angle into which the incident particle is scattered.

In the center of mass system

$$\frac{d |p_I|}{dE} = \frac{E_{IF} E_{SF}}{c^2 p_I (E_{IF} + E_{SF})} \quad (15)$$

(14) is integrated over E first

$$\sigma = \frac{N^2}{4\pi^2 c^3 \hbar^4} \int \frac{(\bar{U}_{IF} K U_{IO})^2 P_I E_{IF} E_{SF}}{(E_{IF} + E_{SF})} d\Omega_I \quad (16)$$

(13) implies that

$$d\Omega_I \sim \left[ \Delta p + \frac{2\hbar\pi}{N^{1/3}a} \right]^2 \frac{1}{P_{IO}^2}$$

The integral (16) is over all values of  $\Omega$  which approximately conserve energy and momentum as implied by the integrations (13) and (14). (16) may approach  $N^2$  times the cross section of a single particle on one site.

The result (16) was obtained for the very simple cubic model. A similar result may be obtained for any very tightly bound group of scatterers, even if these are not arranged in a perfect periodic lattice.

### Discussion

The large cross sections (16) result from three very important assumptions. The ensemble of scatterers is assumed to be infinitely stiff, and recoils in the same manner as a single elementary particle on the N sites. Expression (6) then states

that a final ensemble state differs from an initial state only in the phase factor  $e^{i\Delta p r X/\hbar}$ . This phase factor is crucial for obtaining a large cross section because it may enormously increase the solid angle into which scattering occurs.

Suppose first that the phase factor  $e^{i\Delta p r X/\hbar}$  is absent -- as in the published solutions<sup>7</sup> for potential scattering -- in which energy but not momentum is conserved. The absence of  $\Delta p$  may enormously decrease the value of (16), because under this condition (13) implies (center of mass system),

$$\frac{N^{1/3} a (p_{I0} - p_{IF})}{2\hbar} \ll \pi \quad (17)$$

(17) then limits the solid angle into which scattering may occur, expression (16), to

$$\Delta \Omega < \left( \frac{2\hbar\pi}{N^{1/3} a} \right)^2 \frac{1}{p_{I0}^2} = \left[ \frac{2\pi \text{ (De Broglie wavelength of incident particle)}}{\text{length of scatterer array}} \right]^2 \quad (18)$$

The limitation of the  $\Omega$  integration by (17) results in an

extremely small cross section. This limit disappears when the phase factor  $e^{i\Delta p_r x^r/\hbar}$  is included, for  $\Delta p_r$  the same value for all scatterers.

This follows from the modification of (17) as a result of the collective momentum transfer phase shift, to

$$\Delta \Omega < \left[ \Delta p + \frac{2\frac{1}{2}\pi}{N^{1/3}a} \right]^2 \frac{1}{(p_{10})^2} \quad (19)$$

For large N, if  $\Delta p \rightarrow p_{10}$ , (19) is enormously greater than (18). The cross section (16) and transition probabilities are correspondingly increased.

The second assumption is that the ensemble consists of highly localized particles which do not, therefore, have well defined momenta. It can be shown that if the momenta of all scatterers are precisely known before and after the interaction with the incident beam, the total cross section (and transition probability) will be very small.

The third assumption is that the sign of the interaction is the same in all volume elements. For electromagnetic radiation incident on a solid, this requires an applied nearly uniform field to obtain essentially the same polarization in all volume elements. For the neutrino field, the universal Fermi interaction has the same sign for all particles of the solid.

## Coherent Scattering of Neutrinos and Antineutrinos

Let us apply (16) to the scattering of neutrinos by a crystal. The neutral current interaction then gives

$$\sigma = \frac{G_W^2 N^2}{4\pi^2 \hbar^4 c^4} \int E_\nu^2 \langle (\bar{U}_{\nu 0} \gamma^\alpha (1 + \gamma_5) U_{\nu 0} \bar{U}_{\nu F} \gamma_\alpha (1 + \gamma_5) U_{\nu 0})^2 \rangle d\Omega_\nu \quad (20)$$

It is possible to show<sup>8</sup> that

$$\bar{U}_{\nu 0} \gamma^\alpha (1 + \gamma_5) U_{\nu 0} U_{\nu F} \gamma_\alpha (1 + \gamma_5) U_{\nu 0} = \bar{U}_{\nu 0} \gamma^\alpha (1 + \gamma_5) U_{\nu 0} \bar{U}_{\nu F} \gamma_\alpha (1 + \gamma_5) U_{\nu 0} \quad (21)$$

In "spinor" representation

$$\gamma_5 = \begin{vmatrix} -1 & 0 \\ 0 & 1 \end{vmatrix} \quad \bar{\gamma} = \begin{vmatrix} 0 & -\bar{\sigma} \\ \bar{\sigma} & 0 \end{vmatrix} \quad (22)$$

All elements here are 2 x 2 matrices

$$\bar{\gamma} (1 + \gamma_5) = \begin{vmatrix} 0 & -2\bar{\sigma} \\ 0 & 0 \end{vmatrix} \quad (23)$$

Let

$$U_3 = \begin{vmatrix} \eta_3 \\ \chi_3 \end{vmatrix} \quad U_2 = \begin{vmatrix} \eta_2 \\ \chi_2 \end{vmatrix} \quad (24)$$

$\eta$  and  $\chi$  are 2 component spinors

$$\bar{U}_3 \bar{r}(1+r_3)U_3 = -2 \chi_3^* \bar{\sigma} \chi_3 \quad (25)$$

$$\bar{U}_3 r^0(1+r_3)U_3 = 2 \chi_3^* \chi_3 \quad (26)$$

therefore

$$\frac{G_M \bar{U}_3 r^0(1+r_3)U_2 \bar{U}_2 r_2(1+r_3)U_3}{\sqrt{2}} = \frac{4G_M}{\sqrt{2}} \left[ \chi_{SF}^* \chi_{SO} \chi_{VF}^* \chi_{VO} - \chi_{SF}^* \bar{\sigma} \chi_{SO} \cdot \chi_{VF}^* \bar{\sigma} \chi_{VO} \right] \quad (27)$$

For unpolarized scatterers, the last (spin terms) in (27) would be expected to average to zero.

Suppose the incident direction is the z direction. For

scattering through an angle  $\theta$ , the spinor transformation law leads to\*

$$\chi'_{\nu f} \chi_{\nu 0} = \cos \frac{\theta}{2} \quad (28)$$

Integration of (20) then gives for the total cross section

$$\sigma = \frac{4G_W^2 E_\nu^2 N^2}{\pi \hbar^4 c^4} \quad (29)$$

#### Experimental Checks

We expect (29) to be valid at low energies because available materials are expected to behave as "infinitely stiff" only for momentum transfer  $p$  satisfying the requirement

$$p^2 \ll 2MkT_D \quad (30)$$

In (30),  $M$  is the mass of a scatterer,  $k$  is Boltzmann's constant, and  $T_D$  is the Debye temperature.

\* (28) is the same for both neutrinos and antineutrinos. In general, if all terms in 27 contribute significantly, the neutrino and antineutrino cases would not be identical.

An experiment has been carried out to directly observe the coherent scattering. A titanium tritide source was employed in a stainless steel thin walled container. The target was a single crystal of sapphire 2.5 centimeters in diameter and 0.38 cms thick.

(30) is easily met. The antineutrinos have an average energy of 13 kilovolts and the Debye temperature of sapphire is approximately 1000 Kelvin. The torsion balance of Figure 1 was employed.

## Apparatus

A closed loop servosystem was developed to measure the forces exerted on the crystals. A radiofrequency bridge became unbalanced whenever the torsion balance was displaced from its equilibrium position. The unbalance voltage was amplified, and then employed to produce an electrostatic force to restore the balance to equilibrium. The voltage required to restore the balance to its equilibrium position then measured the force.

The torsion balance was enclosed by a hollow cylinder 20 cm in diameter, about 50 cm high, and maintained at a pressure of  $10^{-6}$  torr by a Vac Ion pumping system.

Two small diameter aluminum cylinders extended from the top of the apparatus into the region close to the target crystals. The outside diameter of the cylinders was 16 mm and the wall thickness was 1.5 mm. The inner region of the cylinders was open to the atmosphere and the lower end was sealed with a welded disk. A motor driven gear train was employed to raise and lower a titanium tritide anti-neutrino source in one cylinder and an identical untritiated "dummy" in the second cylinder.

For initial experiments, the servosystem had an averaging time of about forty seconds. One series of experiments was carried out with closest approach (center of mass to center of mass) of about 22 mm between tritium source and target crystal. A second series was carried out with closest approach approximately one centimeter.

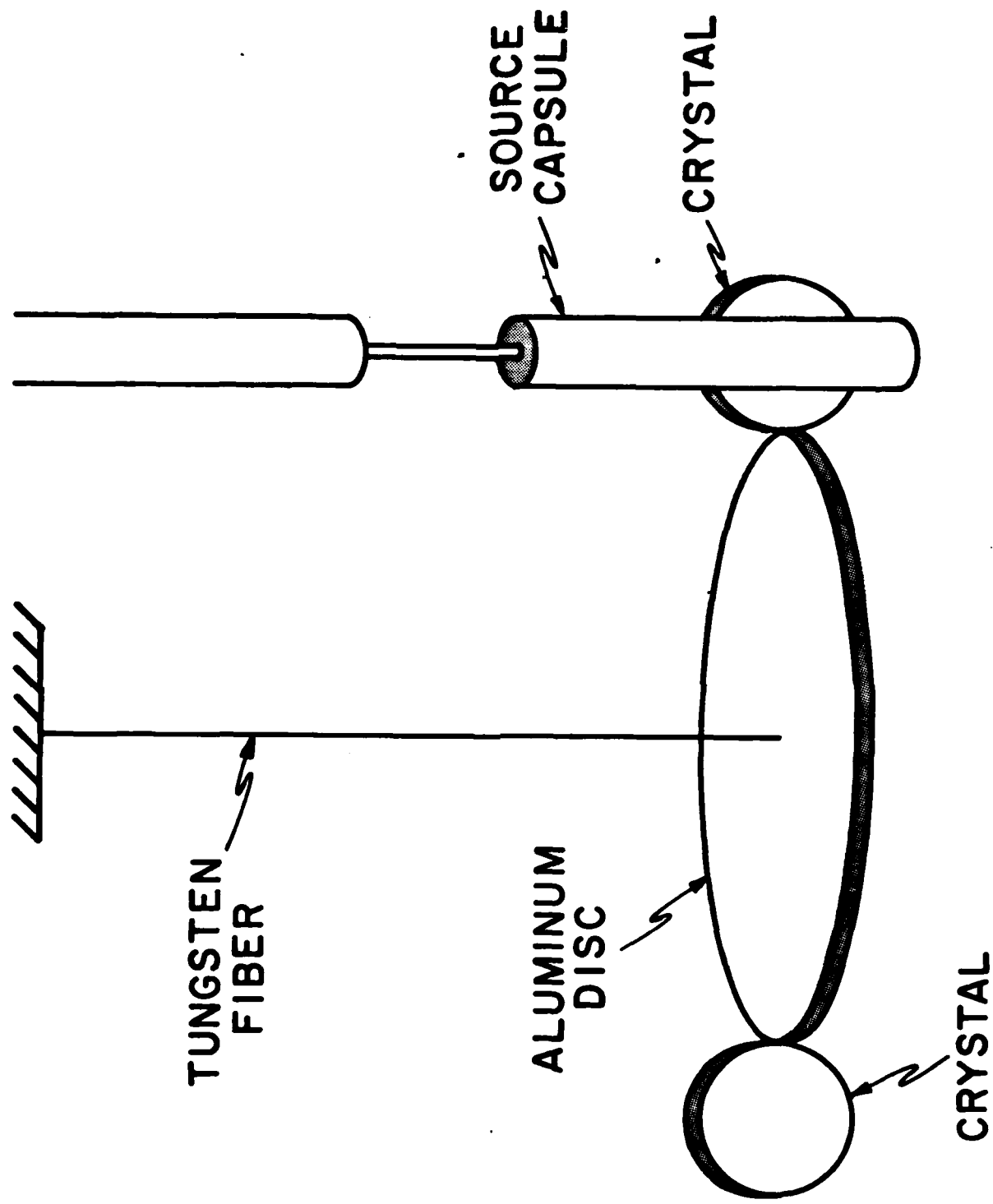


Figure 1

The tritium source was then removed and replaced with a lead mass in one cylinder and nothing in the other cylinder. The gravitational interaction of the lead mass and target crystal then provided a calibration of the torsion balance.

A 1000 Curie tritium source generates considerable heat, about .03 watts, due to the Beta electrons. To assess the effects of insertion of a heat source into the torsion balance, a small resistance was inserted into the "dummy", and coupled to an external low frequency alternating potential. On a time scale of minutes, a .03 watt heat source produced torsion balance servosystem output voltages comparable with the most optimistic expectations for antineutrino scattering. Possible hypotheses for the origin of the thermal effect implied that most of the effect should change sign when the heat source was moved from one small cylinder to the other one. Experiments disclosed that within limits of experimental error the entire thermal effect did change sign when the heat source was moved from one small cylinder to the other one. This made it possible to do null experiments, compensating both the gravitational effect of the tritium source and the thermal effect by a heated "dummy" on the other side of the torsion balance.

Three additional changes were made to reduce the thermal effect to a level comparable with other errors. The small cylinders were enclosed in several layers of superinsulation and the servosystem response time was reduced to nine seconds. The greatly increased diameter of the superinsulated cylinders made it impossible to assemble the torsion balance for cylinder axis distances from the target crystal center smaller than 22 mm. The aluminum disk supporting the target crystals was reduced in mass to achieve greater thermal

isolation of the tungsten wire which supports the target crystal assembly.

### Operation of the Experiments

Let us suppose that there is no interaction between source and target, as the source is lowered into position. Suppose that the interaction is switched on suddenly at the point of closest approach, with torsion balance at rest. An extremum is expected at an elapsed time corresponding to the servosystem response, plus half the torsion balance period. This follows because the solution for displacement  $x$  and velocity  $\dot{x}$ , for a harmonic oscillator at rest  $t = 0$ , driven by a force  $F$  starting at  $t = 0$  is

$$x = \frac{F}{k} \left[ 1 - e^{-\gamma t} \left( \cos \omega t + \frac{\gamma}{\omega} \sin \omega t \right) \right] \quad (31)$$

$$\dot{x} = \frac{\omega F}{k} \left( 1 + \frac{\gamma^2}{\omega^2} \right) e^{-\gamma t} \sin \omega t \quad (32)$$

Clearly the largest value for  $x$  occurs at  $\omega t = \pi$ .

Figure 2 shows a computer drawn output voltage response for a 27gm lead mass which is cycled up and down in the following way. At zero time a motor is started by a pulse which is also written on magnetic tape. The motor drives the gear train, lowering the lead mass nearly to the bottom of the small cylinder in closest approach to the target crystal, in 11 seconds. At 32 seconds, another pulse starts the motor to raise the lead mass to its original position.

Figure 3 is for an 8.6 gram mass at the same distances as Figure 2. Figure 4 is for the same mass and distances as Figure 3, at another time when the noise

background was relatively large, at one third scale of Figure 3. Figure 5 is for the 27 gm lead mass at approximately twice the closest approach distance of the data of Figure 2.

The minimum at 15 seconds in Figure 2 is believed due to the gravitational attractive force between lead mass and target crystal. The interaction force is present at all times, increasing by roughly a factor 100 from the highest to the lowest position of the lead mass. If the interaction were switched on suddenly at the point of closest approach the extremum would be expected to occur at  $23\frac{1}{2}$  seconds. This corresponds to eleven seconds for the mass to travel from top to bottom,  $3\frac{1}{2}$  seconds for a half period of the torsion balance, and nine seconds for the servosystem response. Since the interaction starts long before the mass reaches the end of its travel, an earlier extremum than  $23\frac{1}{2}$  seconds is reasonable.

The peak observed at 42 seconds in Figure 2 is believed due to the lead mass being moved away from the target crystal. If the interaction were suddenly switched off at 32 seconds, an extremum would be expected at one half torsion balance period ( $3\frac{1}{2}$  seconds) plus servosystem response time of 9 seconds, or  $44\frac{1}{2}$  seconds. The occurrence of the extremum at an earlier time may be due to effects of the initial values of position and velocity of the balance. The eleven second time required to raise or lower the mass implies that the time of  $32-11 = 21$  seconds elapses between application of the maximum force and its removal. 43 seconds then elapses between beginning of the upward motion of the lead mass and the recycled lowering again to the closest approach distance. The system e folding time is approximately 30 seconds. Therefore, the occurrence

of the second extremum is much more dependent on the initial values of position and velocity than the occurrence of the first extremum.

Figure 6 shows a computer drawn response to the tritium neutrino source and dummy, for closest approach distance corresponding to that for the lead mass experiment of Figure 4, without drift or other corrections. Figure 7 shows an average over several periods of observation. The error bars refer to the peak measured values and do not include other sources of error.

The peak at about 19 seconds is believed due to the repulsive force associated with the coherent scattering of antineutrinos. The trough at about 44 seconds is believed due to the removal of the neutrino source from the vicinity of the target crystals. The later occurrence of the first repulsive force extremum, compared with the lead mass attractive force extremum, is believed associated with the different dependence of force on distance for the two experiments. The gravitational interaction for two spheres would depend on the inverse square of the distance between centers. In these experiments a lead cylinder interacts with a disk and other masses on the balance. Some departure from an inverse square center to center distance is expected. The tritium source is also a cylinder with a much smaller height than the lead mass. The flux incident on the target crystal depends on the solid angle subtended by the crystal at the source. Because of the orientation factors, this varies more rapidly with center to center distance than an inverse square dependence. For this reason the forces associated with the antineutrinos are believed to increase more rapidly with decreasing distance than the lead mass, giving rise to an extremum corresponding to a closer approach to the target, at the later time. Detailed analyses of the response functions, taking all filtering into account, are being carried out.

Figure 8 shows a computer drawn response for tritium source and dummy with four times the heat input to the "dummy" than present in the tritium source. If the thermal effects were dominant, the peak at 19 seconds and minimum at 44 seconds would have reversed signs as in Figure 2.

### Results

Calorimetric measurements gave a value  $600 \pm 150$  Curies for the neutrino source, in December 1982. The Oak Ridge National Laboratory had prepared a 3000 Curie titanium tritide source ten months earlier. This consists of a tritiated titanium sponge inside a stainless steel cylinder one cm in diameter with wall thickness 0.8 mm. The stainless steel plus the aluminum cylinder walls are believed sufficient to bring all Beta decay electrons to rest. These have kinetic energy less than 20 kilovolts.

The half life of tritium is about 12 years. The observed loss of activity on a time scale of months may be due to destruction of the titanium tritide chemical bonds as a result of bombardment by the Beta decay electrons. If we assume an exponential decay law the activity during the periods associated with Figures 6, 7, and 8 is believed to be  $900 \pm 250$  Curies.

Let  $\langle |p_{\nu t}| \rangle$  be the average momentum transferred by an anti-neutrino to the crystal, and let  $\langle |p_{\nu}| \rangle$  be the average magnitude of the antineutrino momentum. For elastic scattering

$$\langle |p_{\nu t}| \rangle = \frac{\int \langle |p_{\nu}| \rangle (1 - \cos \theta) \cos^2 \frac{\theta}{2} \sin \theta \, d\theta}{\int \cos^2 \frac{\theta}{2} \sin \theta \, d\theta} = \langle |p_{\nu}| \rangle \quad (33)$$

Let  $V_v$  be the servosystem output voltage with the antineutrino source and let  $V_G$  be the servosystem output with the lead mass interacting with the crystal, in each case at the distance of closest approach. Let  $G$  be Newton's constant of gravitation,  $6.6 \times 10^{-8}$  dyne  $\text{cm}^2 \text{gm}^{-2}$ . Let  $A$  be the target area, let  $\Phi$  be the number of antineutrinos per second per unit solid angle. Let  $r_G$  be the distance of closest approach for the lead mass and let  $r_v$  be the distance of closest approach for the antineutrino source, in each case from the center of mass of the target to the axis of the cylinder into which antineutrino source and lead mass are lowered. Let  $m_l$  be the mass of the lead weight and let  $m_c$  be the mass of the target crystal.

$$\langle |p_v| \rangle = \langle |p_{v+l}| \rangle \approx \frac{G m_l m_c V_v r_v^2 K}{\Phi A V_G r_G^2} \quad (34)$$

$$G_g = 6.7 \times 10^{-8} \text{ DYNE CM}^2 \text{ GM}^{-2}$$

$$m_l = 26.98 \text{ GM}$$

$$m_c = 12.73 \text{ GM}$$

$$V_v = 0.14 \text{ VOLTS}$$

$$V_G = .078 \text{ VOLTS}$$

$$r_v \approx r_G \approx 22 \text{ mm}$$

$$\Phi \approx 2.5 \times 10^{12}$$

$$A \approx 5.1 \text{ CM}^2$$

$K$  IS A CORRECTION FOR THE GRAVITATIONAL INTERACTION OF THE LEAD MASS WITH THE BALANCE MASS WHICH SUPPORTS THE CRYSTAL

These values give for the observed antineutrino momentum transfer

$$\langle |P_{\nu}| \rangle \approx (5.1 \pm 2) \times 10^{-19} \text{ GM CM SEC}^{-1} \quad (35)$$

For zero rest mass antineutrinos with average kinetic energy 12.2

KeV the average momentum  $\langle |P_{\nu}| \rangle$  is given by  $6.5 \times 10^{-19} \text{ GM CM SEC}^{-1}$

The implication is that essentially all incident antineutrinos are scattered. Expression (29) gives a result much larger than the area of the crystal. This implies that most of the scattering occurs in about the first ten percent of the crystal depth.\*

#### Conclusion

The observed repulsive force suggests that coherent scattering of antineutrinos is being observed in these experiments.

#### Acknowledgements

This research was supported in part by the Advanced Research Projects Agency (DOD) monitored by the Air Force Office of Scientific Research under Contract F-49620-81-C-0024.

The torsion balance was designed by Mr. Frank DesRosier and the electronics were designed by Mr. J. Kimball. Mr. G. Wilmot prepared the computer programs and analyzed the magnetic tapes.

It is my pleasure to acknowledge very enlightening discussions of the theory with M. H. Mayer, O. W. Greenberg, J. Sucher, J. C. Pati, and C. S. Woo.

---

\*If this is true, the result (35) is reduced by approximately 20 per cent.

AVERAGE SIGNAL 309 21 41 57.2

FIRST HALF MEAN - 05297      SECOND HALF MEAN - 05297

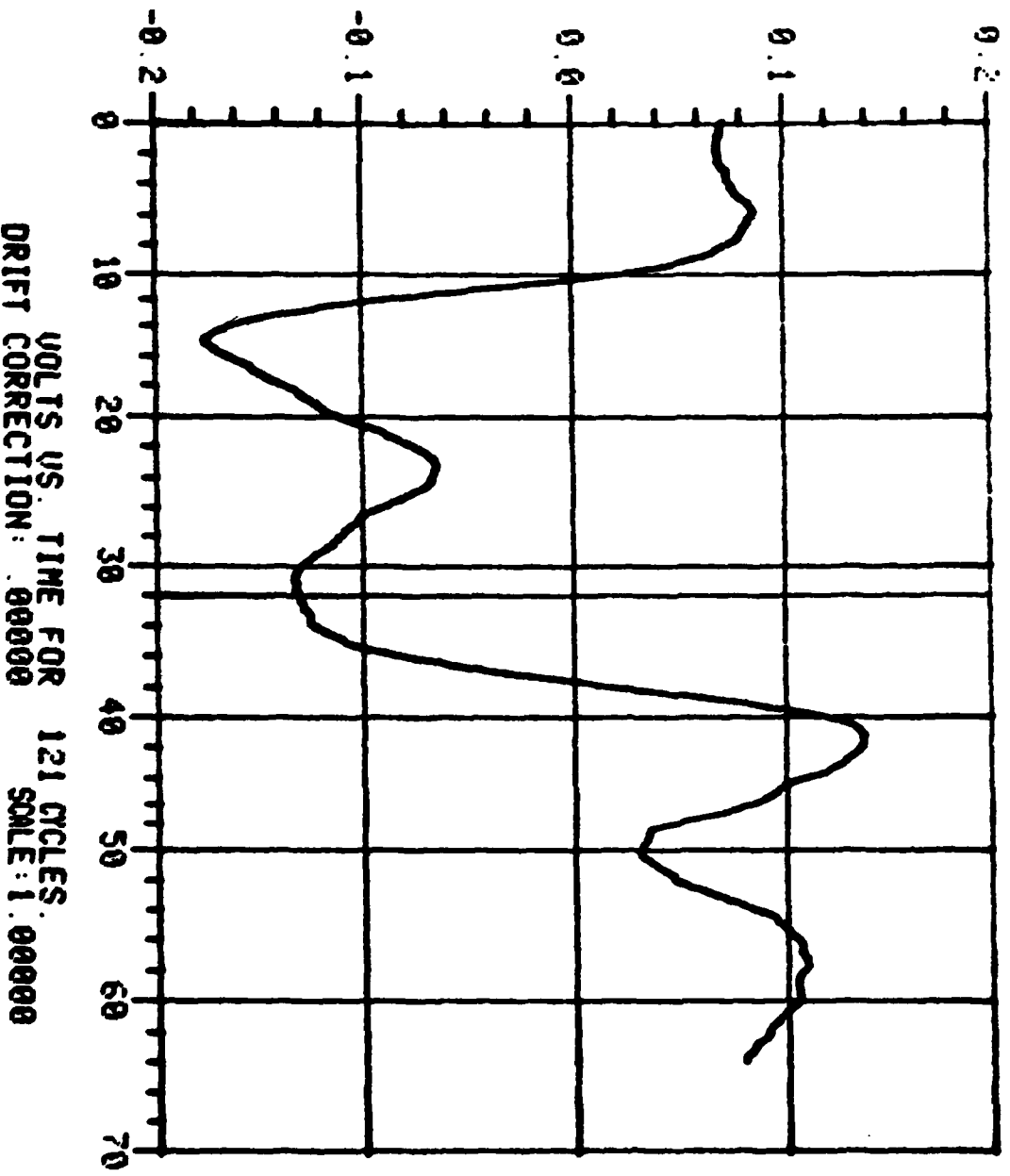
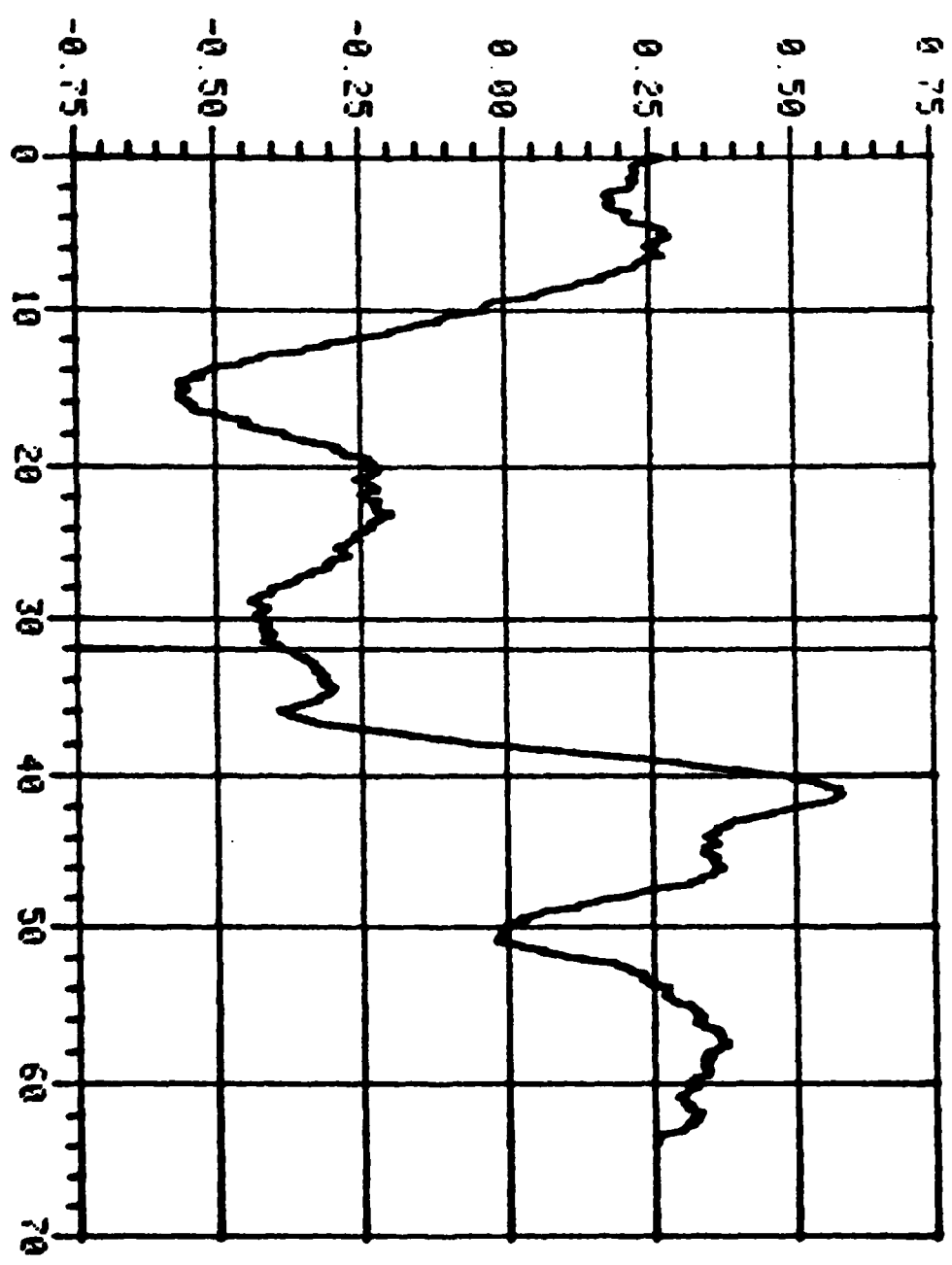


Figure 2

AVERAGED SIGNAL 321 14 1 21 0

$\times 10^{-1}$  FIRST HALF MEAN - 01751 SECOND HALF MEAN . 01750

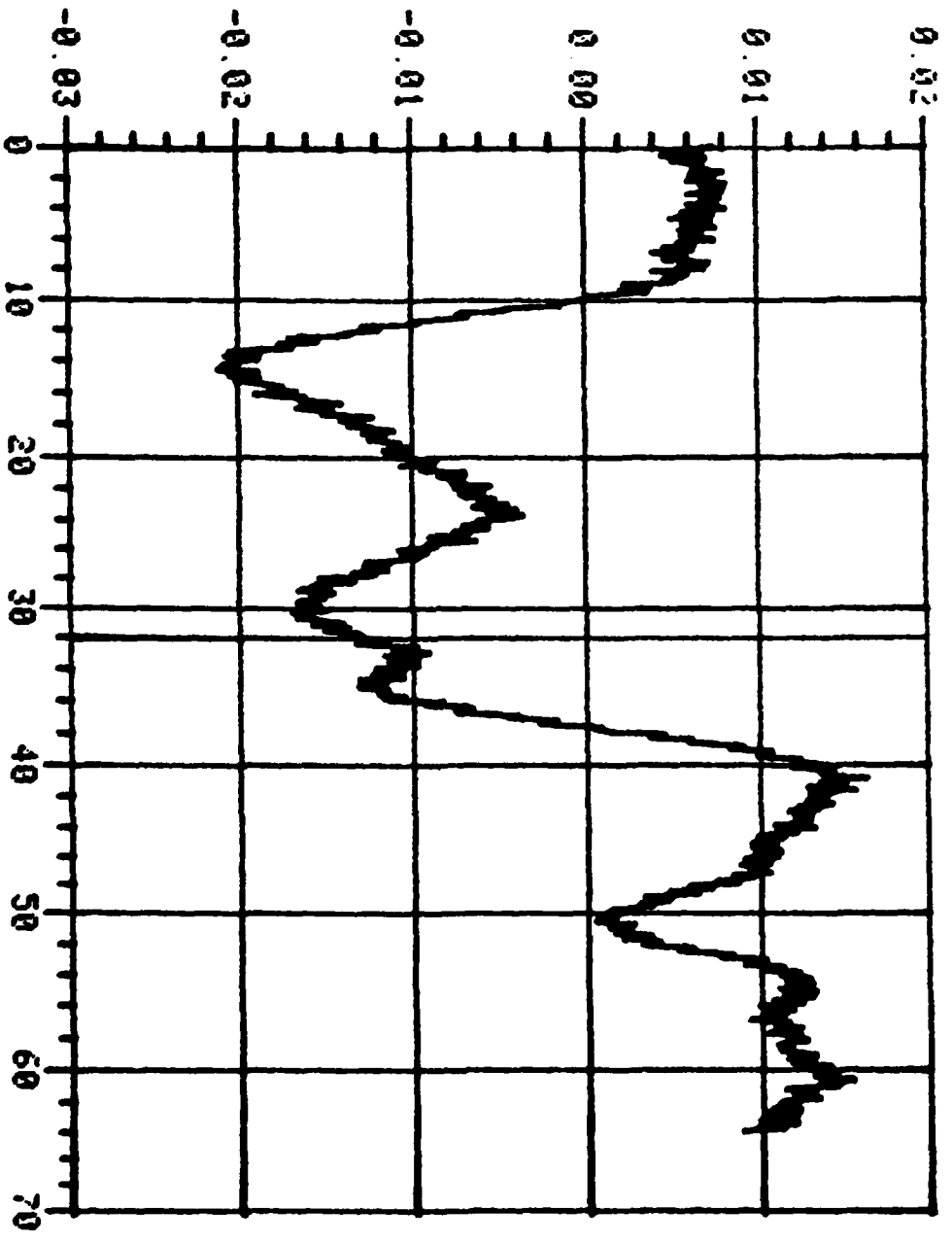


VOLTS VS. TIME FOR 123 CYCLES.  
DRIFT CORRECTION: 00000 SCALE: 1.00000

Figure 3

AVERAGED SIGNAL: 320 23:36:32.0

FIRST HALF MEAN: .00642 SECOND HALF MEAN: .00642



SMALL LEAD

VOLTS VS. TIME FOR 182 CYCLES.  
DRIFT CORRECTION: .00000 SCALE: 1.00000

Figure 4

AVERAGED SIGNAL: 362 21:35:22.2 FILE#4  
FIRST HALF MEAN: -03265 SECOND HALF MEAN: .03265

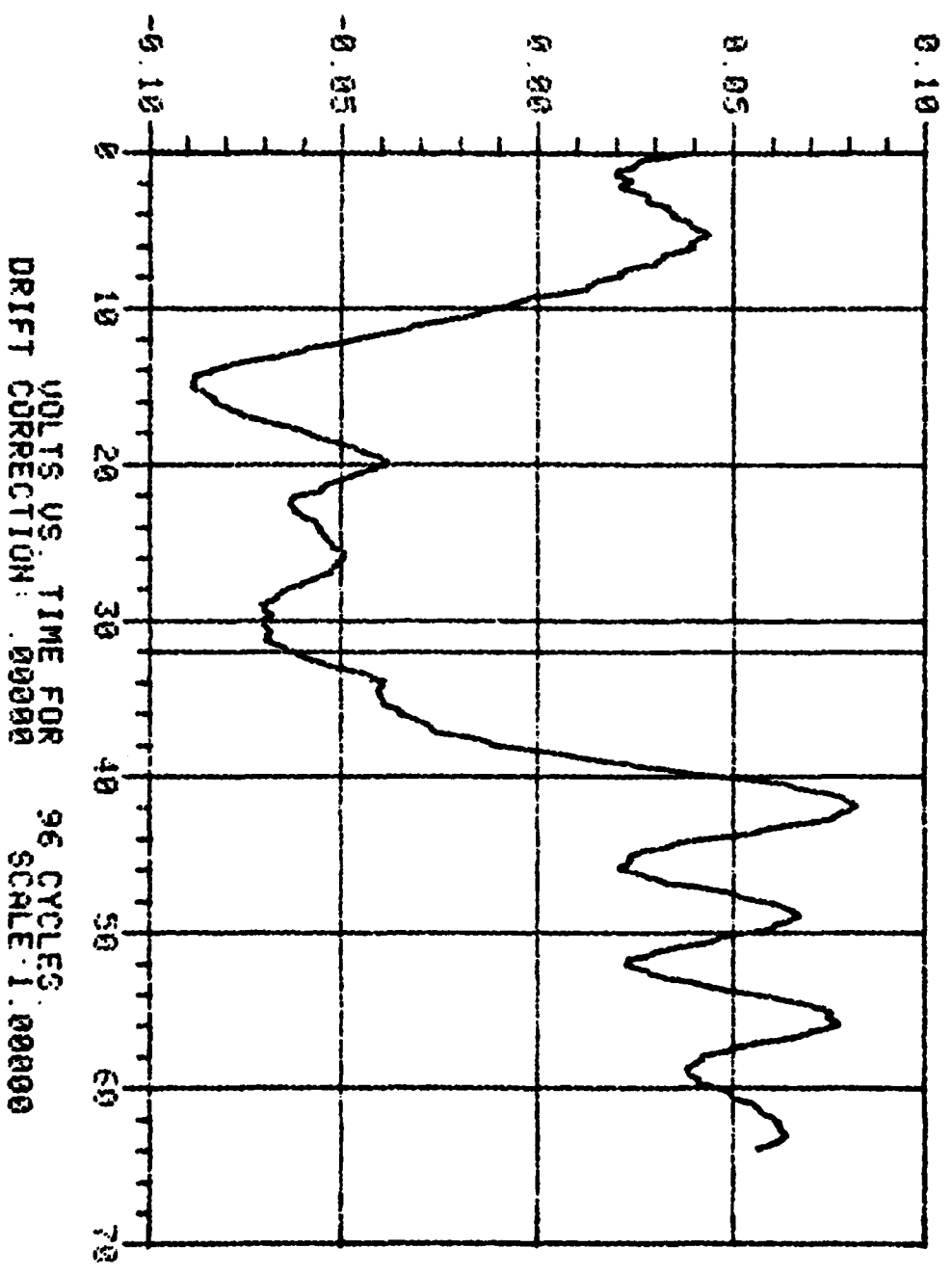


Figure 5

AVERAGED SIGNAL: 282 14:12:21.0 'N'  
FIRST HALF MEAN: .00487 SECOND HALF MEAN: -.00487

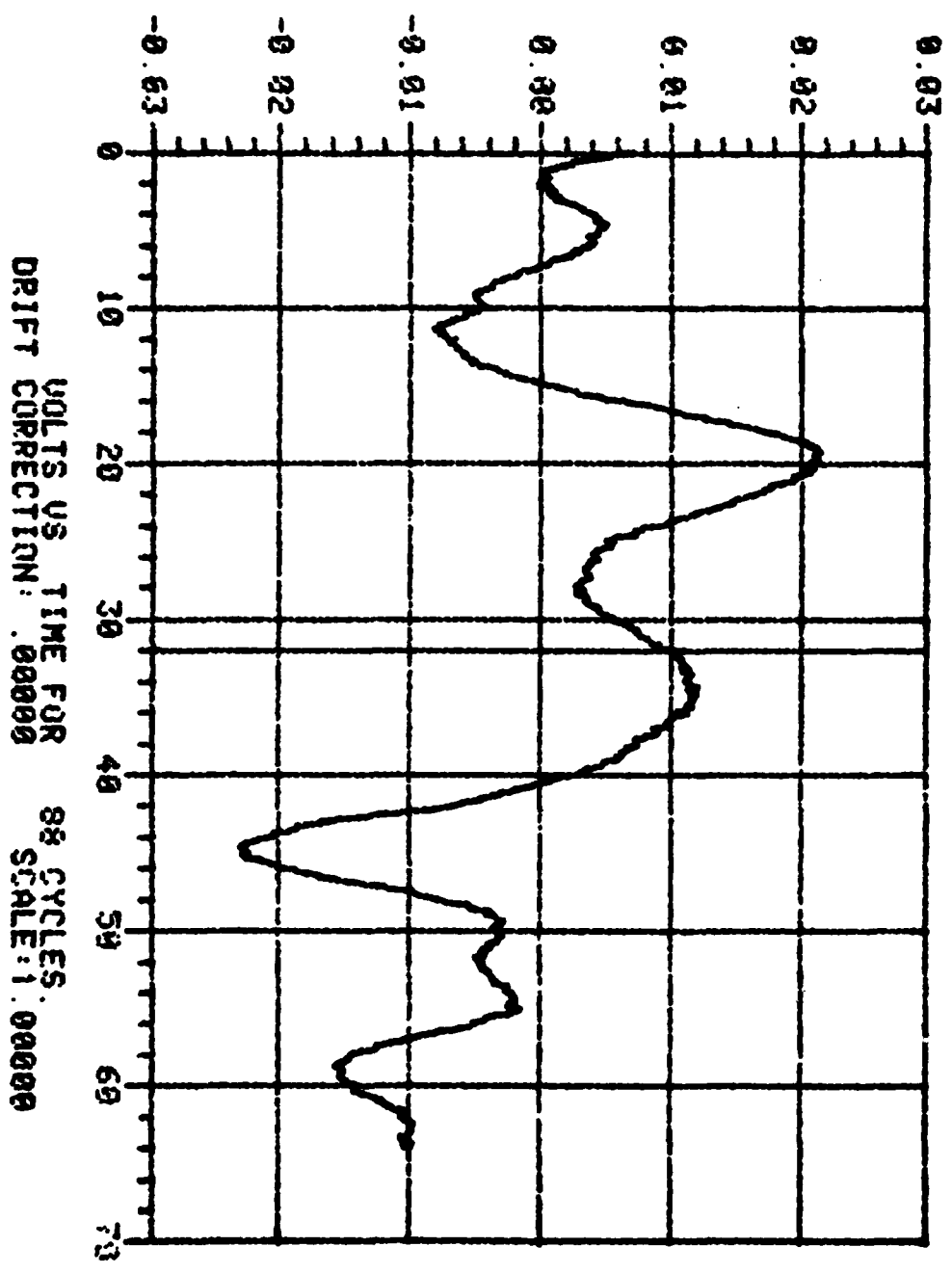


Figure 6

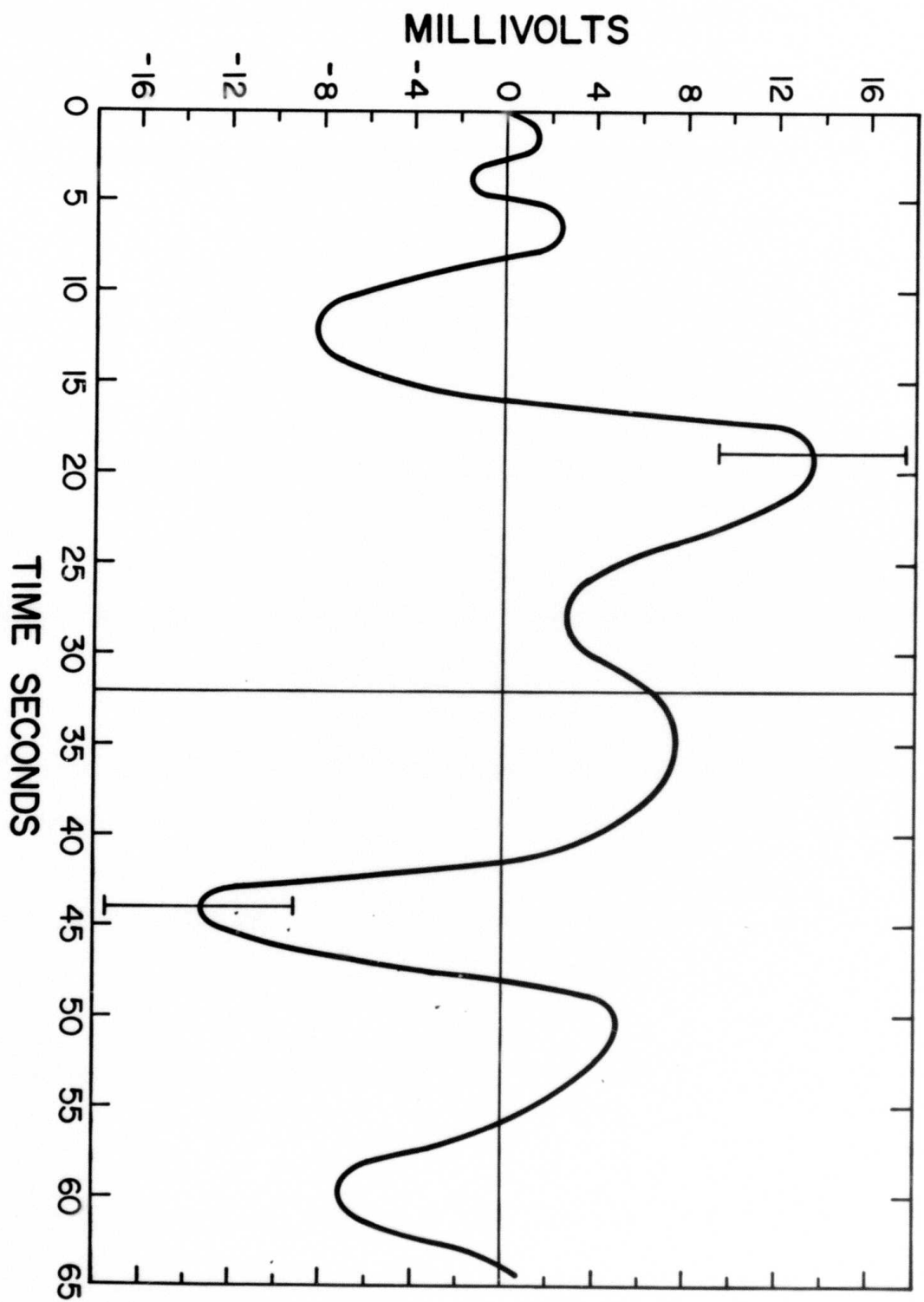
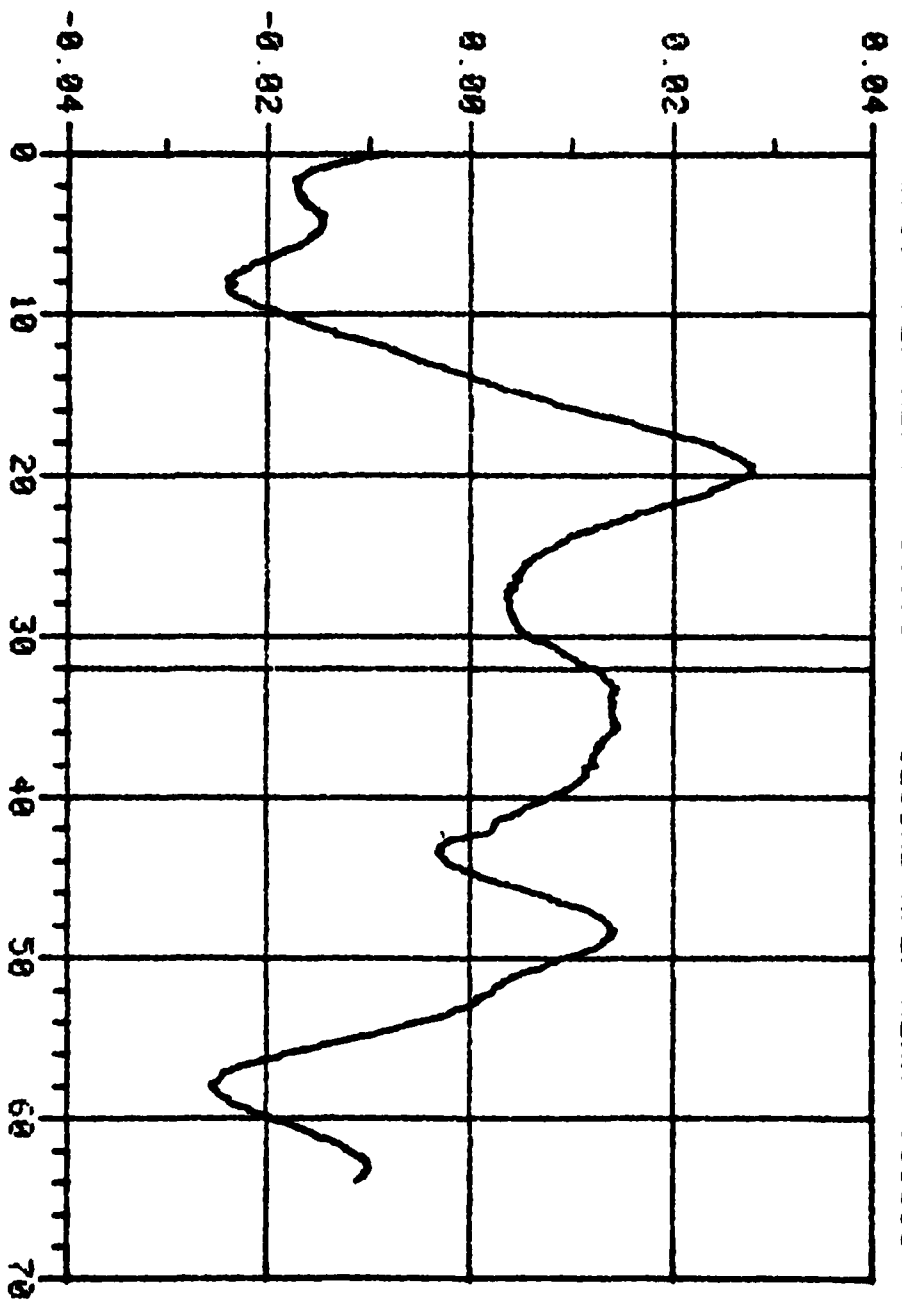


Figure 7

AVERAGED SIGNAL: 283 12:50:22.0 'A'

FIRST HALF MEAN: .00006 SECOND HALF MEAN: -.00006



DRIFT CORRECTION: .00000  
VOLTS US. TIME FOR 141 CYCLES.  
SCALE: 1.00000

SKIPPED 'BAD' CYCLES 1W2,1W2,1W2

Figure 8

## Figure Captions

Figure 1. Torsion Balance for Weak Interaction Experiments

Figure 2. Output Voltage for Gravitational Interaction of 27 gm Lead Mass with Target Crystal ( 11 mm)

Figure 3. Output Voltage for Gravitational Interaction of 8.6 gm Lead Mass with Target Crystal ( 11 mm)

Figure 4. Output Voltage for Gravitational Interaction of 8.6 gm Lead Mass with Target Crystal ( 11 mm ,at 1/3 scale)

Figure 5. Output Voltage for Gravitational Interaction of 27 gm Lead Mass with Target Crystal ( 22 mm)

Figure 6. Output Voltage for Interaction of Tritium Source with Target Crystal, without Drift Correction

Figure 7. Output Voltage for Interaction of Tritium Source with Target Crystal, Averaged over All Runs

Figure 8. Output Voltage for Interaction of Tritium Source, Untritiated "Dummy" with Heat Input of 0.12 Watts, with Target Crystals

<sup>1</sup>A. H. Compton and S. K. Allison, X Rays in Theory and Experiment, Second Edition 1935, page 189, D. Van Nostrand Company, Inc., New York.

<sup>2</sup>This follows from integration of formula 14.114 page 681 of Classical Electrodynamics by J. D. Jackson, Second Edition 1975, John Wiley and Sons, New York, London.

<sup>3</sup>This follows from integration of formula 14.115 page 681 of reference 2.

<sup>4</sup>Landau and Lifshitz, Quantum Mechanics - Non Relativistic Theory, Addison Wesley, Volume 3, 1958, page 215.

<sup>5</sup>Relativistic Quantum Theory Part 2, Chapter XV, E. M. Lifshitz and L. P. Pitaevski 1974, Pergamon Press Ltd., Particle Physics, An Introduction, Chapter VI, M. Leon, Academic Press, 1973.

<sup>6</sup>H. Frauenfelder, The Mossbauer Effect, W. A. Benjamin, Inc., New York 1962.

<sup>7</sup>Relativistic Quantum Theory Part 1, page 214, V. B. Berestetskii, E. M. Lifshitz, and L. P. Pitaevski, 1971, Pergamon Press Ltd.

<sup>8</sup>Relativistic Quantum Theory Part 1, page 88, V. B. Berestetskii, E. M. Lifshitz, and L. P. Pitaevski, 1971, Pergamon Press Ltd.

9. R. J. Mossbauer, Z. Physik 151, 124 (1958); Naturwissenschaften 45, 538 (1958); Z. Naturforsch 14a, 211 (1959).
10. W. E. Lamb Jr., Phys. Rev. 55, 190, 1939.

APPENDIX A

Coherent Scattering With Well Defined Scatterer Momenta

It is sufficient to consider the more simple S matrix.

$$S = \frac{1}{\hbar c} \int \langle F | \bar{\Psi}_S \Psi_S \bar{\Psi}_I K \Psi_I | 0 \rangle d^4x \quad A(1)$$

For well defined scatterer momenta, it is convenient to discuss the elastic scattering case in terms of the center of mass motion.

The following kinds of quantum states are chosen for the operators

$\bar{\Psi}_S$  and  $\bar{\Psi}_I$ .

$$\bar{\Psi}_S = \sum_n \sum_j \bar{\Psi}_{sj}(\vec{r}) a_j^\dagger \Psi_{scn}^*(\vec{r}_c) b_n^\dagger \quad A(2)$$

$$\bar{\Psi}_I = \sum_k \bar{U}_{Ik} e^{-\frac{i\vec{p}_{Ik} \cdot \vec{r}}{\hbar}} d_k^\dagger \left( \frac{1}{\sqrt{V}} \right)$$

In A(2)  $\vec{r}$  is the position three vector,  $a_j^\dagger$  is a creation operator for the state with wavefunction  $\bar{\Psi}_{sj}$ .  $b_n^\dagger$  is a creation operator for the center of mass state with wavefunction  $\Psi_{scn}^*(\vec{r}_c)$ .  $\vec{r}_c$  is the center of mass position three vector.  $d_k^\dagger$  is a creation operator for an incident particle with known momentum  $\vec{p}_{Ik}$ .  $\bar{U}_{Ik}$  may be a scalar, tensor, or spinor required to describe the incident particles.

The wavefunctions  $\Psi_{scn}^*$  for the center of mass are then  $e^{-\frac{i\vec{p}_c \cdot \vec{r}}{\hbar}}$  and the three space part of the integral A(1) may be written as

$$S_3 \rightarrow \bar{U}_{IF} K U_{IO} \int \psi_{SJF}^*(\bar{r}) \psi_{SJO}(\bar{r}) e^{\frac{i}{\hbar} [(\bar{p}_{CO} - \bar{p}_{CF}) \cdot \bar{r}_c + (\bar{p}_{IO} - \bar{p}_{IF}) \cdot \bar{r}]} d\bar{r} d\bar{r}_c \quad A(3)$$

$\bar{p}_{CO}$  and  $\bar{p}_{IO}$  are the original momenta of the center of mass and incident particle respectively, and  $\bar{p}_{CF}$ ,  $\bar{p}_{IF}$  are the final state values. Let  $\bar{r}'$  be the 3 vector from the center of mass to the 3 volume element  $d\bar{r}$ .

$$\bar{r}_c = \bar{r} - \bar{r}' \quad A(4)$$

Substituting A(4) into A(3) and carrying out the integration gives

$$S_3 \rightarrow \bar{U}_{IF} U_{IO} \int \delta_3(\bar{p}_{CO} - \bar{p}_{CF} + \bar{p}_{IO} - \bar{p}_{IF}) \int \psi_{SJF}^*(\bar{r}') \psi_{SJO}(\bar{r}') e^{-\frac{i}{\hbar} (\bar{p}_{IO} - \bar{p}_{IF}) \cdot \bar{r}'} d\bar{r}' \quad A(5)$$

The quantity  $\Delta \bar{p}_r = \bar{p}_{CO} - \bar{p}_{CF}$  will then disappear in the subsequent integrations.

For elastic scattering the "internal" state  $\psi_{SJ}(\bar{r}')$  is not changed by the scattering and  $\psi_{SJF}^*(\bar{r}') = \psi_{SJO}^*(\bar{r}')$ . In practice A(5) will give an extremely small total cross section, because the solid angle into which scattering may occur is limited as in (17)

## Appendix B

### SOME KINEMATICAL CONSIDERATIONS FOR ZERO REST MASS PARTICLES

Suppose a beam of zero rest mass particles is scattered by a large crystal with mass  $M$ , initially at rest. If momentum and energy are strictly conserved and the internal degrees of freedom of  $M$  are not excited, it may be shown that

$$\frac{1}{|P_{IF}|} - \frac{1}{|P_{IO}|} - \frac{1}{Mc} \left( 1 - \sqrt{1 - \frac{p_s^2}{P_{IF}^2} (1 - \cos^2 \varphi)} \right) = 0 \quad (B1)$$

$$P_{IF}^2 - P_{IO}^2 - p_s^2 + 2|P_{IO}||p_s| \cos \varphi = 0 \quad (B2)$$

In (B1) and (B2), following earlier definitions  $P_{IF}$ ,  $P_{IO}$  refer to the final and original incident particle momenta, and  $p_s$  refers to the final momentum of the center of mass of  $M$ .  $\varphi$  is the angle which  $p_s$  makes with the incident particle momentum. For a given value of  $P_{IO}$  it is clear that  $P_{IF}$  and  $\varphi$  may have a wide range of values. An even wider range is possible in practice, since the interaction time is smaller than the length of  $M$  divided by  $c$  and the internal degrees of freedom of  $M$  may share the energy. (B1) implies, for elastic scattering, that  $|P_{IF}| \approx |P_{IO}|$ , and (B2) requires either  $p_s \approx 0$ , or  $p_s \approx 2|P_{IO}| \cos \varphi$ .  $\varphi$  can therefore vary over a wide range. It follows that there are no serious restrictions on the integration (14).